Finite-part integrals over polygons by an 8-nodes quadrilateral spline finite element

Published version:

DOI:10.1007/s10543-010-0262-8

Chong-Jun Li, Vittoria Demichelis and Catterina Dagnino.
Finite-part integrals over polygons by an 8-node quadrilateral spline finite element. *BIT Numerical Mathematics*, 50, no. 2, 2010, DOI 10.1007/s10543-010-0262-8.

BIT manuscript No.
(will be inserted by the editor)

Finite-part integrals over polygons by an 8-node quadrilateral spline finite element

Chong-Jun Li · **Vittoria Demichelis** · **Catterina Dagnino**

Received: date / Accepted: date

Abstract In this paper we consider the numerical integration on a polygonal domain Ω in $\mathbb{R}^2$ of a function $F(x,y)$ which is integrable except at a point $P_0 = (x_0, y_0) \in \overset{\circ}{\Omega}$, where F becomes infinite of order two. We approximate either the finite-part or the two-dimensional Cauchy principal value of the integral by using a spline finite element method combined with a subdivision technique also of adaptive type. We prove the convergence of the obtained sequence of cubatures. Finally, to illustrate the behaviour of the proposed method, we present some numerical examples.

Keywords Finite part integral · Cauchy principal value · Spline finite element method · Bivariate splines

Mathematics Subject Classification (2000) 65D05 · 65D07 · 65D30 · 65D32

1 Introduction

This paper deals with the numerical evaluation of certain hypersingular integrals on a polygonal domain Ω in $\mathbb{R}^2$, i.e. a domain with the boundary composed of piecewise straight lines.

Work supported by the WWS - World Wide Style Project of University of Torino, funded by the Fondazione CRT of Torino (Italy) and by Science Foundation of Dalian University of Technology (No. SFDUT07001, China).

Chong-Jun Li (Corresponding author)
School of Mathematical Sciences, Dalian University of Technology, Dalian 116024, China
E-mail: chongjun@dlut.edu.cn

Vittoria Demichelis
Department of Mathematics, University of Torino, via C. Alberto, 10 Torino 10123, Italy
E-mail: vittoria.demichelis@unito.it

Catterina Dagnino
Department of Mathematics, University of Torino, via C. Alberto, 10 Torino 10123, Italy
E-mail: catterina.dagnino@unito.it

The above integrals arise in several engineering problems and in particular in applied mechanics ([8] and references therein).

Firstly, we consider the integration of a function $F(x,y)$ on a convex domain D, with F integrable except at a point $P_0 = (x_0, y_0)$ where it becomes infinite of order two. We set P_0 as the origin of polar coordinates (r, θ), with $r = \sqrt{(x-x_0)^2 + (y-y_0)^2}$ and denote by $r = R(\theta)$ the polar equation of the contour of D. Following Tricomi's presentation [10], we suppose

$$F(x,y) = \frac{\phi(\theta)}{r^2} + F_1(x,y), \tag{1.1}$$

where F_1 denotes a function at most infinite of (algebraic) order less than two at isolated points.

We set

$$⨍_D F(x,y)\,dxdy := \int_D F_1(x,y)\,dxdy + \int_0^{2\pi} \phi(\theta)\log R(\theta)\,d\theta. \tag{1.2}$$

If $\int_0^{2\pi} \phi(\theta)\,d\theta = 0$ then (1.2) defines the two-dimensional Cauchy principal value integral [10]; otherwise, it defines the Hadamard finite-part [7].

The numerical evaluation of (1.2), with

$$F(x,y) = \frac{f(x,y)}{r^2} \tag{1.3}$$

and D a triangle, a rectangle or, more in general, a convex polygon, has been studied in literature.

A classical approach consists in the decomposition of D in triangles, each one with the singular point P_0 at one vertex. Then, the integral on each triangle is evaluated by a cubature rule of sufficiently high degree of exactness.

Since P_0 is the origin of polar coordinates, $f(x,y)$ can be expressed by

$$f(x,y) = f(x_0 + r\cos\theta, y_0 + r\sin\theta) = \bar{f}(r,\theta). \tag{1.4}$$

Cubatures based on product of univariate Gaussian rules on each triangle of the decomposition of D, are proposed in [6]. Convergence results are proved for $\bar{f}(r,\theta) \in H^s_{\mu,\mu}$, $s \geq 1$, $0 < \mu \leq 1$, where $H^s_{\mu,\mu}$ denotes the space of functions with continuous partial derivatives up to the order s and such that each partial derivative of order s satisfies a Hölder condition of order μ, i.e.

$$|\bar{f}^{(s)}(\bar{r},\bar{\theta}) - \bar{f}^{(s)}(r,\theta)| \leq C(|\bar{r} - r|^\mu + |\bar{\theta} - \theta|^\mu), \quad C > 0. \tag{1.5}$$

Approximations for (1.2), based on local bivariate quadratic quasi-interpolating splines on each triangle of the decomposition of D, are studied in [1], where convergence results are proved for $\bar{f}(r,\theta)$ satisfying the condition (1.5), with $s = 0$.

Gaussian rules and bivariate splines are combined in [11] for evaluating

$$⨍_D \frac{g(P_0,\theta)}{r^p}\Phi(P)\,dP, \quad p = 2,3,$$

where D is a rectangle. Convergence results are proved assuming that $g(P_0,\theta)$ is continuous and $\Phi(P) \in \mathbb{C}^{p+2}(D)$.

In this paper, we consider the problem of the numerical evaluation of

$$I = \oint_{\Omega} F(x,y)\,dxdy, \quad P_0 \in \overset{\circ}{\Omega}, \tag{1.6}$$

where Ω is a not necessarily convex polygonal domain and F is defined by (1.3) with $f(x,y) \in \mathbb{C}(\Omega \setminus P_0)$.

We propose a method based on a special spline quadrilateral finite element ([3, 12]), reproducing all bivariate polynomials of total degree at most two, and applied by a subdivision technique also of adaptive kind.

We denote by D a convex subset of Ω, such that the singular point $P_0 \in \overset{\circ}{D}$. If $\overline{f}$, given by (1.4), satisfies the following condition on D

$$\left|\overline{f}(r,\theta) - \overline{f}(0,\theta)\right| \le A(\theta) r^{\nu}, \quad 0 < \nu \le 1, \quad 0 \le A(\theta) < \infty, \tag{1.7}$$

then we can express F on D in the form (1.1), with

$$\phi(\theta) = \overline{f}(0,\theta) \text{ and } F_1(x,y) = \frac{\overline{f}(r,\theta) - \overline{f}(0,\theta)}{r^2}. \tag{1.8}$$

We set $I = I_1 + I_2$, where $I_1 = \oint_D F(x,y)\,dxdy$ is defined by (1.2), with F_1 and ϕ given in (1.8), and $I_2 = \int_{\Omega \setminus D} F(x,y)\,dxdy$, with F defined by (1.3), is a regular integral. We evaluate I_2 by the cubature formula over polygons, having degree of exactness 2 [5] and based on the spline finite element method presented in [3], combined with the subdivision technique also of adaptive kind ([4]). Then, we apply the same finite element method to evaluate I_1.

For $\overline{f}$ satisfying the condition (1.7), we prove the convergence to I of the obtained cubature sequence. Such condition is weaker than conditions on f required by previous methods in $[1,6,11]$.

The above performances make our composite strategy suitable when $\overline{f}(r,\theta)$ and $f(x,y)$ are not smooth in D and $\Omega \setminus D$, respectively, for example with singularities of the gradient. Moreover, the adaptive subdivision technique concentrates nodes in regions of difficulty, reducing the computational cost with respect to a non adaptive one. However, when Ω is a convex polygon and $\overline{f}(r,\theta)$ is a smooth function, our composite strategy cannot be competitive with more classical ones, based on high degree polynomial approximation at Gaussian.

The integration nodes of our method lie on the boundary of each quadrilateral element and, in the subdivision procedure, they are shared by several elements, i.e. the subdivision procedure generates an embedded sequence of integration nodes. This feature makes the computational cost of our method lower than that one of another similar composite strategy, using a basic (polynomial) interpolatory type cubature, whose interior nodes are not kept in the procedure of subdivision, as remarked in [5].

The paper is organized as follows. In Section 2 we review some results related to the spline finite element method and to the cubature for regular integrals based on it. In Section 3 we present the cubature for (1.6), we analyse the convergence and we discuss its computational cost. Finally, Section 4 proposes some numerical examples illustrating the behaviour of our cubatures. Some structural characteristics of our algorithm and a possible extension to other cases of singular integrals are also discussed.

2 L8 spline operator and cubature

In this section, we review some results on the interpolation operator and cubature by L8 element basis presented in [3] and [5].

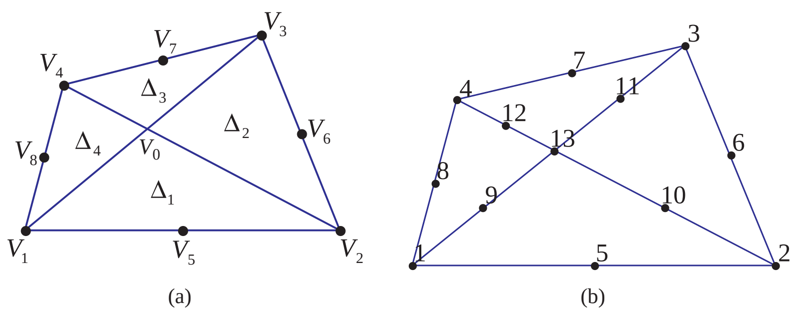

Fig. 2.1 The 8 nodes and 13 domain points on a quadrilateral element.

For a convex quadrilateral element Q, divided by four triangles $\Delta_1,\ldots,\Delta_4$ as shown in Fig. 2.1(a), we consider the eight nodes $V_1,\ldots,V_8$, where

$$V_5=(V_1+V_2)/2,\ V_6=(V_2+V_3)/2,\ V_7=(V_3+V_4)/2,\ V_8=(V_4+V_1)/2,$$

and the quadratic spline space defined on the quadrangle Q, with C^1 smoothness on both diagonals $\overline{V_1V_3}$ and $\overline{V_2V_4}$. The dimension of the spline space is eight, as given in [3].

It is well known ([2]) that a polynomial p of total degree two on a triangle Δ can be represented in the local Bernstein basis as

$$p(\lambda)=\sum_{|\alpha|=2}\gamma_\alpha b_\alpha(\lambda)$$

where $b_\alpha(\lambda)=\frac{2}{\alpha!}\lambda^\alpha$, $\lambda=(\lambda_1,\lambda_2,\lambda_3)$ are the barycentric coordinates of Δ, $\alpha=(\alpha_1,\alpha_2,\alpha_3)$, $|\alpha|=\alpha_1+\alpha_2+\alpha_3=2$, $\alpha!=\alpha_1!\alpha_2!\alpha_3!$ and $\lambda^\alpha=\lambda_1^{\alpha_1}\lambda_2^{\alpha_2}\lambda_3^{\alpha_3}$. The γ_α are called *Bézier ordinates or Bézier coefficients* of p. The points with barycentric coordinates $\alpha/2$ are called domain points in Δ. The piecewise linear interpolant to the points $(\alpha/2,\gamma_\alpha)$ is called *Bézier net* or *B-net* or *control net* of p. Such a B-net uniquely defines the patch, a fact which is made use of in the so called Bernstein-Bézier technique, where all information about the patch is extracted from this net.

Then, by the B-net method, there are thirteen domain points in the quadrilateral element, as shown in Fig. 2.1(b). We denote by L8 basis the eight quadratic nodal basis splines $L_i\,(i=1,\ldots,8)$ interpolating the eight nodes $V_1,\ldots,V_8$, ([3]). The Bézier coefficients of each base $L_i\,(i=1,\ldots,8)$, according to the thirteen domain points, are given in the following matrix

$$(L_1\,L_2\,L_3\,L_4\,L_5\,L_6\,L_7\,L_8)^T$$
$$= \begin{pmatrix} 1 & 0 & 0 & 0 & -\frac{1}{2} & 0 & 0 & -\frac{1}{2} & -\frac{1}{2} & -\frac{b}{2} & 0 & -\frac{b}{2} & -\frac{b}{2} \\ 0 & 1 & 0 & 0 & -\frac{1}{2} & -\frac{1}{2} & 0 & 0 & -\frac{a}{2} & -\frac{1}{2} & -\frac{a}{2} & 0 & -\frac{a}{2} \\ 0 & 0 & 1 & 0 & 0 & -\frac{1}{2} & -\frac{1}{2} & 0 & 0 & -\frac{d}{2} & -\frac{1}{2} & -\frac{d}{2} & -\frac{d}{2} \\ 0 & 0 & 0 & 1 & 0 & 0 & -\frac{1}{2} & -\frac{1}{2} & -\frac{c}{2} & 0 & -\frac{c}{2} & -\frac{1}{2} & -\frac{c}{2} \\ 0 & 0 & 0 & 0 & 2 & 0 & 0 & 0 & 2a & 2b & 0 & 0 & 2ab \\ 0 & 0 & 0 & 0 & 0 & 2 & 0 & 0 & 0 & 2d & 2a & 0 & 2ad \\ 0 & 0 & 0 & 0 & 0 & 0 & 2 & 0 & 0 & 0 & 2c & 2d & 2cd \\ 0 & 0 & 0 & 0 & 0 & 0 & 0 & 2 & 2c & 0 & 0 & 2b & 2bc \end{pmatrix}$$

where a,b,c,d are defined by the following ratios:

$$a = \frac{|\overline{V_4V_0}|}{|\overline{V_4V_2}|},\ b = \frac{|\overline{V_3V_0}|}{|\overline{V_3V_1}|},\ c = 1-a,\ d = 1-b. \tag{2.1}$$

The spline basis consists of piecewise quadratic polynomials $\mathbb{C}^1$ continuous on the two diagonals and $\mathbb{C}^0$ on the boundary of Q. By the barycentric coordinates in each triangle, it is easy to obtain the piecewise polynomial form $L_i(x,y)$, $i=1,\ldots,8$ in Cartesian coordinates by the above B-net form.

The Fig. 2.2 shows the representations in Cartesian coordinates of the L8 basis on $[-1,1]^2$.

The interpolation operator by the L8 basis on Q is defined by ([3])

$$L_Q f(x,y) = \sum_{i=1}^{8} f(V_i^Q) L_i^Q(x,y), \tag{2.2}$$

where V_i^Q and $L_i^Q(x,y)$ $(i=1,2,\ldots,8)$ are the eight nodes V_i and basis splines $L_i(x,y)$ defined on Q specifically. $L_Q f(x,y)$ interpolates f at the eight nodes and reproduces polynomials of degree two ([3]), i.e.,

$$L_Q f(V_i^Q) = f(V_i^Q),\ i=1,\ldots,8,$$

and

$$L_Q f = f,\ \forall f \in \mathbb{P}_2.$$

Since $L_Q f \in \mathbb{C}^1(Q)$, it is easy to obtain its partial derivatives. In particular, when $Q=[-1,1]^2$, then $V_0=(0,0)$, $V_1=(-1,-1)$, $V_2=(1,-1)$, $V_3=(1,1)$, $V_4=(-1,1)$. Let $f_i=f(V_i)$, $i=1,\ldots,8$, then $L_{[-1,1]^2} f(x,y)=\sum_{i=1}^8 f_i L_i(x,y)$, where $L_i(x,y)$ are shown in Fig. 2.2 in piecewise polynomial form. Differentiating the polynomials in Fig. 2.2 at $V_i(i=0,1,\ldots,4)$, we obtain the values of the first partial derivatives of $L_{[-1,1]^2} f$ at $V_0,V_1,\ldots,V_4$, as shown in Table 2.1.

Then, for a polygonal domain Ω, divided by N convex quadrilateral elements Q_k $(k=1,\ldots,N)$, the L8 cubature on Ω is defined by ([5])

$$\tilde{I}_\Omega f = \sum_{k=1}^{N} \tilde{I}_{Q_k} f,$$

Δ_1

$\frac{1}{4}(-1+x+2x^2+y+3xy+2y^2)$
$\frac{1}{4}(-1-x+2x^2+y-3xy+2y^2)$
$-\frac{1}{4}(1+x)(1+y)$
$\frac{1}{4}(-1+x)(1+y)$
$\frac{1}{2}(1-2x^2-2y-y^2)$
$\frac{1}{2}(1+2x-y)(1+y)$
$\frac{1}{2}(1+y)^2$
$-\frac{1}{2}(1+y)(-1+2x+y)$

Δ_2

$-\frac{1}{4}(-1+x)(-1+y)$
$\frac{1}{4}(-1-x+2x^2+y-3xy+2y^2)$
$\frac{1}{4}(-1-x+2x^2-y+3xy+2y^2)$
$\frac{1}{4}(-1+x)(1+y)$
$-\frac{1}{2}(-1+x)(1+x-2y)$
$\frac{1}{2}(1+2x-x^2-2y^2)$
$-\frac{1}{2}(-1+x)(1+x+2y)$
$\frac{1}{2}(-1+x)^2$

Δ_3

$-\frac{1}{4}(-1+x)(-1+y)$
$\frac{1}{4}(1+x)(-1+y)$
$\frac{1}{4}(-1-x+2x^2-y+3xy+2y^2)$
$\frac{1}{4}(-1+x+2x^2-y-3xy+2y^2)$
$\frac{1}{2}(-1+y)^2$
$-\frac{1}{2}(-1+y)(1+2x+y)$
$\frac{1}{2}(1-2x^2+2y-y^2)$
$-\frac{1}{2}(-1+y)(1-2x+y)$

Δ_4

$\frac{1}{4}(-1+x+2x^2+y+3xy+2y^2)$
$\frac{1}{4}(1+x)(-1+y)$
$-\frac{1}{4}(1+x)(1+y)$
$\frac{1}{4}(-1+x+2x^2-y-3xy+2y^2)$
$-\frac{1}{2}(1+x)(-1+x+2y)$
$\frac{1}{2}(1+x)^2$
$-\frac{1}{2}(1+x)(-1+x-2y)$
$\frac{1}{2}(1-2x-x^2-2y^2)$

Fig. 2.2 The piecewise polynomials of L8 basis on each triangles $\Delta_1,\dots,\Delta_4$ in $[-1,1]^2$.

Table 2.1 The partial derivatives of $L_{[-1,1]^2} f$ at $V_0, V_1, \dots, V_4$.

	V_0	V_1	V_2	V_3	V_4
$\frac{\partial}{\partial x}$	$\frac{f_1-f_2-f_3+f_4+4f_6-4f_8}{4}$	$\frac{4f_5-3f_1-f_2}{2}$	$\frac{f_1+3f_2-4f_5}{2}$	$\frac{3f_3+f_4-4f_7}{2}$	$\frac{4f_7-f_3-3f_4}{2}$
$\frac{\partial}{\partial y}$	$\frac{f_1+f_2-f_3-f_4-4f_5+4f_7}{4}$	$\frac{4f_8-3f_1-f_4}{2}$	$\frac{4f_6-3f_2-f_3}{2}$	$\frac{f_2+3f_3-4f_6}{2}$	$\frac{f_1+3f_4-4f_8}{2}$

where

$$\tilde{I}_{Q_k} f = \int_{Q_k} L_{Q_k} f(x,y)dxdy = \sum_{i=1}^{8} C_i^{Q_k} f(V_i^{Q_k}). \tag{2.3}$$

The coefficients $C_i^Q = \int_Q L_i^Q(x,y)dxdy$, with $Q = Q_k$ $(k = 1,\dots,N)$, can be computed as follows:

$$\begin{aligned}
C_1^Q &= -\tfrac{1}{6}b(S_1+S_2+S_3+S_4),\\
C_2^Q &= -\tfrac{1}{6}a(S_1+S_2+S_3+S_4),\\
C_3^Q &= -\tfrac{1}{6}d(S_1+S_2+S_3+S_4),\\
C_4^Q &= -\tfrac{1}{6}c(S_1+S_2+S_3+S_4),\\
C_5^Q &= \tfrac{1}{3}((1+a+b+ab)S_1+(b+ab)S_2+abS_3+(a+ab)S_4),\\
C_6^Q &= \tfrac{1}{3}((d+ad)S_1+(1+a+d+ad)S_2+(a+ad)S_3+adS_4),\\
C_7^Q &= \tfrac{1}{3}(cdS_1+(c+cd)S_2+(1+c+d+cd)S_3+(d+cd)S_4),\\
C_8^Q &= \tfrac{1}{3}((c+bc)S_1+bcS_2+(b+bc)S_3+(1+b+c+bc)S_4),
\end{aligned} \tag{2.4}$$

where $S_1,\dots,S_4$ are the areas of the four triangles $\Delta_1,\dots,\Delta_4$ in $Q = Q_k$ and a,b,c,d are defined in (2.1).

It is clear that the formula (2.3) and its coefficients (2.4) only depend on the four vertices V_i^Q, $i=1,\dots,4$. In particular, if Q is a rectangle or a parallelogram with area S_Q then ([5])

$$\begin{array}{l} a=b=c=d=\frac{1}{2}, \quad S_1=S_2=S_3=S_4=\frac{S_Q}{4} \quad \text{and} \\ C_1^Q=C_2^Q=C_3^Q=C_4^Q=-\frac{1}{12}S_Q, \quad C_5^Q=C_6^Q=C_7^Q=C_8^Q=\frac{1}{3}S_Q. \end{array} \tag{2.5}$$

The cubature is exact for quadratic polynomials on arbitrary convex quadrangulations, and for cubic polynomials on rectangulations ([5]).

3 The algorithm for finite-part integral evaluation on a polygonal domain

We consider integrals of the form (1.6) for $F(x,y)$ defined by (1.3), with $f(x,y) \in \mathbb{C}(\Omega \setminus P_0)$. In order to evaluate (1.6), we use the following subdivision strategy.

1) The whole polygonal domain Ω is divided into several initial quadrilateral elements, where the singular point P_0 is at the center of a square element D_0, as shown in Fig. 3.1(a).
2) In subdivision, the square D_0 is divided into one small square D_1 and four symmetric trapezoidal elements, as shown in Fig. 3.1(b) and so on, step by step, obtaining the squares $D_k \subset D_{k-1} \subset \cdots \subset D_0$.
3) Each quadrilateral element, except the square D_k, is divided into two or four quadrilateral elements by equal subdivision or adaptive subdivision [4].

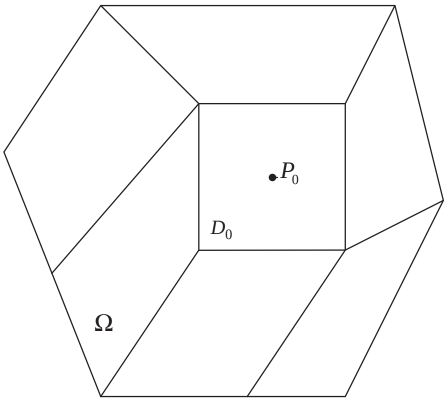

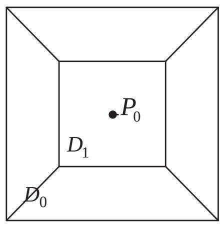

Fig. 3.1 A domain with singular point and initial quadrilateral elements.

Denote by $D_0 = P_0 + [-h_0, h_0]^2$ the square with edge $2h_0$ and $P_0 = (x_0, y_0)$ as center, where h_0 is a positive constant such that $D_0 \subset \Omega$. Then the contour of D_0 is

$$R_0(\theta) = \begin{cases} \frac{-h_0}{\sin\theta}, & \theta \in [-\frac{3\pi}{4}, -\frac{\pi}{4}], \\ \frac{h_0}{\cos\theta}, & \theta \in [-\frac{\pi}{4}, \frac{\pi}{4}], \\ \frac{h_0}{\sin\theta}, & \theta \in [\frac{\pi}{4}, \frac{3\pi}{4}], \\ \frac{-h_0}{\cos\theta}, & \theta \in [\frac{3\pi}{4}, \frac{5\pi}{4}]. \end{cases} \tag{3.1}$$

Set $D_k = P_0 + [-h_k, h_k]^2$, where $h_k = h_0/2^k$, $k = 1, 2, \ldots$. Denote by $R_k(\theta)$ the contour of D_k, obtained by replacing h_0 by h_k in (3.1).

The above subdivision includes one square D_k and other quadrilateral elements in the quadrangulation of $\Omega \setminus D_k = \{\Omega \setminus D_0\} \cup \{D_0 \setminus D_k\}$. Denote by δ the length of the longest diagonal or edge in all elements $Q \subset \Omega \setminus D_k$. Then the subdivision procedure can be described by considering $k \to \infty$ and $\delta \to 0$.

The integral (1.6) can be expressed as follows

$$I = ⨍_{\Omega} \frac{f(x,y)}{r^2} dxdy = I_1 + I_2,$$

where

$$I_1 = ⨍_{D_0} \frac{f(x,y)}{r^2} dxdy$$

and

$$I_2 = \int_{\Omega \setminus D_0} \frac{f(x,y)}{r^2} dxdy.$$

At the kth step, for $k = 1, 2, \ldots$, with reference to I_1, using (1.2) and (1.8), we write

$$\begin{aligned} I_1 &= \int_{D_0} F_1(x,y)\, dxdy + \int_0^{2\pi} \bar{f}(0,\theta) \log R_0(\theta) d\theta \\ &= \int_0^{2\pi} \int_0^{R_k(\theta)} \frac{\bar{f}(r,\theta) - \bar{f}(0,\theta)}{r} dr d\theta + \int_{D_0 \setminus D_k} F_1(x,y) dxdy + \int_0^{2\pi} \bar{f}(0,\theta) \log R_0(\theta) d\theta \\ &= I_{1,1}^{(k)} + I_{1,2}^{(k)} + I_{1,3}, \end{aligned}$$

where $I_{1,3}$ can be computed exactly by

$$\begin{aligned} I_{1,3} &= \int_0^{2\pi} \bar{f}(0,\theta) \log R_0(\theta) d\theta \\ &= \log h_0 \int_0^{2\pi} \bar{f}(0,\theta) d\theta - \int_{-\pi/4}^{\pi/4} \sum_{i=-1}^{2} \bar{f}(0, \theta + \frac{i\pi}{2}) \log \cos\theta d\theta, \end{aligned} \tag{3.2}$$

since $R_0(\theta)$ is fixed and given in Eq. (3.1).

Integrals $I_{1,1}^{(k)}$, $I_{1,2}^{(k)}$ and I_2 can be computed numerically by the spline interpolation operator L_Q defined in (2.2) on each quadrilateral element Q of the quadrangulation on $\Omega \setminus D_k$, as follows.

In order to evaluate $I_{1,1}^{(k)}$, we approximate $\bar{f}(r,\theta)$ on the square D_k by

$$L_{D_k} \bar{f}(r,\theta) = \sum_{i=1}^{8} f(V_i^{D_k}) \bar{L}_i^{D_k}(r,\theta), \tag{3.3}$$

where $V_i^{D_k}(i = 1, \ldots, 8)$ are the eight nodes on D_k and $\bar{L}_i^{D_k}(r,\theta)$ $(i = 1, \ldots, 8)$ are the eight basis splines defined on D_k, by replacing x and y by $(x - x_0)/h_k = r\cos\theta/h_k$ and $(y - y_0)/h_k = r\sin\theta/h_k$ in the representations in Fig. 2.2, respectively.

Therefore

$$I_{1,1}^{(k)} \simeq \tilde{I}_{1,1}^{(k)} = \int_0^{2\pi} \int_0^{R_k(\theta)} \frac{L_{D_k} \overline{f}(r,\theta) - L_{D_k} \overline{f}(0,\theta)}{r} dr d\theta = \sum_{i=1}^{8} \hat{C}_i^{(k)} f(V_i^{D_k}), \quad (3.4)$$

where the cubature coefficients are

$$\hat{C}_i^{(k)} = \int_0^{2\pi} \int_0^{R_k(\theta)} \frac{\overline{L}_i^{D_k}(r,\theta) - \overline{L}_i^{D_k}(0,\theta)}{r} dr d\theta. \quad (3.5)$$

By some algebra, it is easy to obtain

$$\{\hat{C}_i^{(k)}\}_{i=1,\dots,8} = \{1,1,1,1,-1,-1,-1,-1\}. \quad (3.6)$$

Hence

$$I_{1,1}^{(k)} \simeq \tilde{I}_{1,1}^{(k)} = \sum_{i=1}^{4} f(V_i^{D_k}) - \sum_{i=5}^{8} f(V_i^{D_k}).$$

In order to evaluate $I_{1,2}^{(k)}$, denoting by N_k the number of quadrilateral elements in the subdivision of $D_0 \setminus D_k$, we write

$$\begin{aligned} I_{1,2}^{(k)} \simeq \tilde{I}_{1,2}^{(k,\delta)} &= \sum_{j=1}^{N_k} \int_{Q_j} L_{Q_j} F_1(x,y) dx dy \\ &= \sum_{j=1}^{N_k} \sum_{i=1}^{8} C_i^{Q_j} F_1(V_i^{Q_j}), \end{aligned} \quad (3.7)$$

where $C_i^{Q_j}$ are the cubature coefficients (2.4) on each element $Q = Q_j \subset D_0 \setminus D_k$.

Finally, denoting by M the number of quadrilateral elements in $\Omega \setminus D_0$,

$$\begin{aligned} I_2 \simeq \tilde{I}_2^{(\delta)} &= \sum_{j=1}^{M} \int_{Q_j} L_{Q_j} F(x,y) dx dy \\ &= \sum_{j=1}^{M} \sum_{i=1}^{8} C_i^{Q_j} F(V_i^{Q_j}), \end{aligned} \quad (3.8)$$

where $C_i^{Q_j}$ are the cubature coefficients (2.4) on each element $Q = Q_j \subset \Omega \setminus D_0$.

In conclusion,

$$I \simeq \tilde{I}^{(k,\delta)} = \tilde{I}_{1,1}^{(k)} + \tilde{I}_{1,2}^{(k,\delta)} + \tilde{I}_2^{(\delta)} + I_{1,3}. \quad (3.9)$$

In order to study the convergence of proposed cubatures, we need the following lemma.

Lemma 3.1 *For any P_0 as the origin of polar coordinates, if (1.7) holds on D_0, then for $k = 1, 2, \dots$*

$$|L_{D_k} \overline{f}(r,\theta) - L_{D_k} \overline{f}(0,\theta)| \leq 8A(\theta) r^{\nu}.$$

Proof By the definition of D_k and the operator L_{D_k} in (3.3), $L_{D_k}\overline{f}(r,\theta) = L_{D_k} f(P) \in \mathbb{C}^1(D_k)$ and $L_{D_k} f(P) = L_{[-1,1]^2} f(\frac{P-P_0}{h_k})$ is a piecewise quadratic polynomial on D_k. Note that only the values of f at the nodes $V_i^{D_k}(i = 1,\dots,8)$ on the boundary of D_K are used in $L_{D_k} f(P)$. Then, by Table 2.1 and assumption conditions we have

$$\begin{aligned}\left\{\left|\frac{\partial L_{D_k} f(P)}{\partial x}\right|, \left|\frac{\partial L_{D_k} f(P)}{\partial y}\right|\right\} &\le \frac{4}{h_k}\max_{i=1,\dots,8}|f(V_i^{D_k}) - \overline{f}(0,\theta)| \\ &\le \frac{4}{h_k}\max_{(r,\theta)\in D_k}|\overline{f}(r,\theta) - \overline{f}(0,\theta)| \\ &\le \frac{4}{h_k}A(\theta)(\sqrt{2}h_k)^{\nu}. \end{aligned} \tag{3.10}$$

Note that $r = |P - P_0| \le \sqrt{2}h_k$, for $P \in D_k$. Therefore, from (3.10)

$$\begin{aligned}&|L_{D_k}\overline{f}(r,\theta) - L_{D_k}\overline{f}(0,\theta)| \\ &\le r\max_{(r,\theta)\in D_k}\left|\frac{\partial L_{D_k} f(r,\theta)}{\partial r}\right| \\ &\le r^{\nu}(\sqrt{2}h_k)^{1-\nu}\max_{P\in D_k}\left|\frac{\partial L_{D_k} f(P)}{\partial x}\cos\theta + \frac{\partial L_{D_k} f(P)}{\partial y}\sin\theta\right| \\ &\le 8A(\theta)r^{\nu}.\end{aligned}$$

□

We state and prove the following convergence result.

Theorem 3.1 *For any $P_0 \in \overset{\circ}{\Omega}$ as the origin of polar coordinates, if $f \in \mathbb{C}(\Omega \setminus P_0)$ and (1.7) holds on D_0, then*

$$\tilde{I}^{(k,\delta)} \to I \text{ as } k \to \infty \text{ and } \delta \to 0. \tag{3.11}$$

Proof Let $E^{(k,\delta)} = |I - \tilde{I}^{(k,\delta)}|$. From (3.9) we can write

$$E^{(k,\delta)} \le E_{1,1}^{(k)} + E_{1,2}^{(k,\delta)} + E_2^{(\delta)},$$

where

$$E_{1,1}^{(k)} = |I_{1,1}^{(k)} - \tilde{I}_{1,1}^{(k)}|, \quad E_{1,2}^{(k,\delta)} = |I_{1,2}^{(k)} - \tilde{I}_{1,2}^{(k,\delta)}|, \quad E_2^{(\delta)} = |I_2 - \tilde{I}_2^{(\delta)}|.$$

From (1.7) and Lemma 3.1,

$$\begin{aligned}E_{1,1}^{(k)} &\le \int_0^{2\pi}\int_0^{R_k(\theta)}\frac{|(\overline{f}(r,\theta) - \overline{f}(0,\theta)) - (L_{D_k}\overline{f}(r,\theta) - L_{D_k}\overline{f}(0,\theta))|}{r}drd\theta \\ &\le \int_0^{2\pi}\int_0^{R_k(\theta)}\frac{A(\theta)r^{\nu} + 8A(\theta)r^{\nu}}{r}drd\theta \\ &\le \int_0^{2\pi}\hat{A}(\theta)\left(\int_0^{R_k(\theta)} r^{\nu-1}dr\right)d\theta \\ &= \int_0^{2\pi}\hat{A}(\theta)(R_k(\theta))^{\nu}/\nu d\theta.\end{aligned}$$

Since $\hat{A}(\theta) = 9A(\theta)$ is bounded and $R_k(\theta) \to 0$ as $k \to \infty$, for any $\varepsilon > 0$, $\exists\, k_0 \in \mathbb{N}$, such that $E_{1,1}^{(k_0)} < \varepsilon/3$.

Then, fix k_0 and D_{k_0}. By the error estimate on the operator L_Q in [5], from (3.7) we have

$$\begin{aligned} E_{1,2}^{(k_0,\delta)} &\le \sum_{j=1}^{N_{k_0}} \int_{Q_j} |F_1(x,y) - L_{Q_j} F_1(x,y)| dxdy \\ &= \int_{D_0 \setminus D_{k_0}} |F_1(x,y) - L_{D_0 \setminus D_{k_0}} F_1(x,y)| dxdy \\ &\le 2\omega_{D_0 \setminus D_{k_0}}(F_1, \delta) \cdot S_{D_0} = 8h_0^2 \omega_{D_0 \setminus D_{k_0}}(F_1, \delta), \end{aligned} \tag{3.12}$$

where

$$L_{D_0 \setminus D_{k_0}} F_1(x,y) = \sum_{j=1}^{N_{k_0}} L_{Q_j} F_1(x,y),$$

$\omega_{D_0 \setminus D_{k_0}}(F_1, \delta)$ is the modulus of continuity of $F_1 \in \mathbb{C}(D_0 \setminus D_{k_0})$, $S_{D_0} = 4h_0^2$ is the area of D_0 and, especially, δ is the length of the longest diagonal or edge in all elements $Q \subset D_0 \setminus D_{k_0}$.

Hence, for the same above ε, $\exists\, \delta_0 > 0$, such that $\omega_{D_0 \setminus D_{k_0}}(F_1, \delta_0) < \varepsilon/(24h_0^2)$. If the subdivision of $D_0 \setminus D_{k_0}$ is such that $\delta < \delta_0$, then from (3.12) we can deduce $E_{1,2}^{(k_0,\delta)} < \varepsilon/3$.

Similarly, from (3.8)

$$\begin{aligned} E_2^{(\delta)} &\le \sum_{j=1}^{M} \int_{Q_j} |F(x,y) - L_{Q_j} F(x,y)| dxdy \\ &= \int_{\Omega \setminus D_0} |F(x,y) - L_{\Omega \setminus D_0} F(x,y)| dxdy \\ &\le 2\omega_{\Omega \setminus D_0}(F, \delta) \cdot S_{\Omega \setminus D_0}, \end{aligned} \tag{3.13}$$

where

$$L_{\Omega \setminus D_0} F(x,y) = \sum_{j=1}^{M} L_{Q_j} F(x,y),$$

$\omega_{\Omega \setminus D_0}(F, \delta)$ is the modulus of continuity of $F \in \mathbb{C}(\Omega \setminus D_0)$, $S_{\Omega \setminus D_0}$ is the area of $\Omega \setminus D_0$ and, especially, δ is the length of the longest diagonal or edge in all elements $Q \subset \Omega \setminus D_0$.

For the same above ε, $\exists\, \delta_1 > 0$, such that $\omega_{\Omega \setminus D_0}(F, \delta_1) < \varepsilon/(6S_{\Omega \setminus D_0})$. If the subdivision of $\Omega \setminus D_0$ is such that $\delta < \delta_1$, then from (3.13) we get $E_2^{(\delta)} < \varepsilon/3$.

In conclusion, for $k > k_0$ and $\delta < \min\{\delta_0, \delta_1\}$, it holds

$$E^{(k,\delta)} < \varepsilon. \tag{3.14}$$

Therefore, (3.11) follows from (3.14). □

Now, we consider the computational cost of our cubature due both to the number of integration nodes in (3.9) and to the construction of its coefficients.

From Fig. 2.1(a) and from the description of our algorithm, it is clear that the subdivision strategy generates an embedded sequence of integration nodes. Consequently, the total number of cubature nodes is $V+E$, where V is the number of the vertices of the quadrangulation, E is the number of the edges, respectively. We outline that the number of function evaluations one has to perform is lower than that one of another similar composite strategy using a basic (polynomial) interpolatory type cubature with nodes interior to each quadrilateral element. Comparisons with the tensor product 2×2 Gauss-Legendre cubature and the tensor product Simpson rule are presented in [5].

With reference to the computational cost due to the construction of the basic rule coefficients, defined either by (2.4), in case of a general quadrilateral element, or by (2.5), in case of rectangles and parallelograms, we can remark that it is comparable with the computational cost of another similar composite strategy applied on quadrilateral elements and based on classical rules, like those ones above mentioned. Indeed, classical basic rules require bilinear transformations from general quadrilateral elements to rectangular ones.

4 Numerical examples and conclusions

In this section, we propose some numerical examples to test our method for integrals of the form (1.6), with F defined by (1.3). We consider several functions f, given in Table 4.1, and two kinds of integration domains Ω: the square $[-1,1]^2$ and the nonconvex polygon in Fig. 4.1.

For $\Omega=[-1,1]^2$ and $f=f_1$, we can compare numerical results of our cubature with those ones presented in [6,9] and obtained by classical methods based on the decomposition of Ω in triangles having a common vertex at P_0 and on tensor product of univariate integration rules.

Table 4.1 The test functions f.

i	$f_i(x,y)=\overline{f_i}(r,\theta)$	F_1
1	$\frac{x-x_0}{r}=\cos\theta$	0
2	$\frac{(x-x_0)e^x}{r}=e^x\cos\theta$	$\frac{(e^x-e^{x_0})\cos\theta}{r^2}$
3	$\frac{r^{3/2}+\lvert x-x_0\rvert}{r}=\sqrt{r}+\lvert\cos\theta\rvert$	$r^{-3/2}$
4	$\sqrt{\lvert x-y\rvert}$	$\frac{\sqrt{\lvert x-y\rvert}-\sqrt{\lvert x_0-y_0\rvert}}{r^2}$

By (3.2), for each function $\overline{f}=\overline{f_i}$ $(i=1,\dots,4)$, the integrals $I_{1,3}$ are

$$\int_0^{2\pi}\overline{f_1}(0,\theta)\log R_0(\theta)d\theta=\int_0^{2\pi}\cos\theta\log R_0(\theta)d\theta=0,$$
$$\int_0^{2\pi}\overline{f_2}(0,\theta)\log R_0(\theta)d\theta=e^{x_0}\int_0^{2\pi}\cos\theta\log R_0(\theta)d\theta=0,$$
$$\int_0^{2\pi}\overline{f_3}(0,\theta)\log R_0(\theta)d\theta=\int_0^{2\pi}|\cos\theta|\log R_0(\theta)d\theta$$

$$
\begin{aligned}
&= 4\log h_0 - \int_0^{\pi/4} 4(\sin\theta + \cos\theta)\log\cos\theta d\theta \\
&= 4\log h_0 - 8\mathrm{arctanh}(\tan\frac{\pi}{8}) + 4, \\
\int_0^{2\pi} \overline{f}_4(0,\theta)\log R_0(\theta)d\theta &= \sqrt{|x_0-y_0|}\int_0^{2\pi}\log R_0(\theta)d\theta \\
&= \sqrt{|x_0-y_0|}(2\pi\log h_0 - 4\int_{-\pi/4}^{\pi/4}\log\cos\theta \mathrm{d}\theta) \\
&= \sqrt{|x_0-y_0|}(2\pi\log(2h_0) - 4Catalan),
\end{aligned}
$$

where $Catalan = \sum_{k=0}^{\infty}(-1)^k(2k+1)^{-2} \simeq 0.915966$ ([14]).

For the function $f = f_1$, we know the following explicit formula of the integral I on $\Omega = [-1,1]^2$ ([6])

$$
\begin{aligned}
I &= \oint_\Omega \frac{f_1(x,y)}{r^2}dxdy \\
&= \log\frac{[1-y_0+\sqrt{(1+x_0)^2+(1-y_0)^2}][-1-y_0+\sqrt{(1+x_0)^2+(1+y_0)^2}]}{[-1-y_0+\sqrt{(1+x_0)^2+(1+y_0)^2}][1-y_0+\sqrt{(1-x_0)^2+(1-y_0)^2}]}
\end{aligned}
$$

and in Table 4.2 we present the relative errors of our cubature (3.9), combined with an equal subdivision, for several singular points P_0. In the Table, 'EleN', 'NodN' and 'Rel-Err' denote the number of elements, the number of nodes and the relative error, respectively. Such results show the convergence of our method.

Then, in order to improve its performance, we combine (3.9) with the adaptive subdivision scheme proposed in [4]. Each quadrilateral element is checked, and the elements with the largest estimated error are selected automatically to be subdivided into two or four sub-elements according to the differences of integrand function values in next step. The termination condition is the successive step error less than the given tolerance. The Table 4.3 shows the results, in terms of relative errors/total number of nodes, when the adaptive algorithm stops with tolerance 10^{-4} and 10^{-5}, where 'Step-Err' and 'Approximate Value' denote the successive step error and the approximate value of the integral, respectively.

We compare the above results with those presented in [6,9]. With reference to numerical results of rules based on tensor product of Gaussian quadratures ([6], Table 2), we note they show a better convergence rate, as we espected, because $\overline{f}_1(r,\theta) = \cos(\theta)$ is a smooth function. With reference to results of rules based on tensor product of composite trapezoidal and Gaussian quadratures ([9], Table 1), the relative errors, with respect to the total number of nodes, seem to be comparable with ours.

However, we can remark that a significant difference of all such cubatures is in the node location. In the classical approach ([6,9]), the node location is fixed and almost all nodes change when the accuracy degree increases. The advantage of our rule with respect to the other considered ones, is that at any step the previous nodes are kept in the subdivision procedure, since they are vertices of the finer quadrilateral subdivision, which the new nodes belong to. Moreover, our method can be efficiently combined with other numerical algorithms based on quadrilateral element boundary nodes. Finally, it is suitable in case of a nonconvex polygonal integration domain

Ω and the adaptive subdivision allows to dynamically concentrate the computational work in the subregions of Ω where the integrand is more irregular.

Table 4.2 $\Omega = [-1,1]^2$, $f = f_1$, (x_0,y_0)= (a) $(0.4,0.1)$, (b) $(0.6,0.2)$, (c) $(0.8,0.4)$, (d) $(0.9,0.9)$.

Equal subdivision					
EleN	NodN	Rel-Err (a)	Rel-Err (b)	Rel-Err (c)	Rel-Err (d)
5	20	1.57E+00	3.30E+00	1.09E+01	4.54E+01
13	44	4.62E-01	9.05E-01	3.11E+00	1.22E+01
29	100	3.78E-02	9.94E-02	2.87E-01	1.36E+00
61	196	1.15E-02	3.82E-02	5.50E-02	4.90E-01
125	404	4.13E-03	1.05E-02	6.06E-02	3.46E-01
253	788	9.74E-04	4.49E-04	1.57E-02	1.43E-01
509	1588	2.75E-04	1.07E-03	6.89E-03	3.74E-02
1021	3124	4.85E-05	1.54E-04	3.26E-05	4.47E-03

Table 4.3 $\Omega = [-1,1]^2$, $f = f_1$, (x_0,y_0)= (a) $(0.4,0.1)$, (b) $(0.6,0.2)$, (c) $(0.8,0.4)$, (d) $(0.9,0.9)$.

Adaptive subdivision with tolerance 10^{-4}					
(x_0,y_0)	EleN	NodN	Rel-Err	Step-Err	Approximate Value
(a)	265	952	1.20E-04	1.54E-05	-1.234431115739747E+00
(b)	281	1020	1.61E-04	1.57E-05	-2.087387475120013E+00
(c)	345	1244	1.39E-04	1.01E-05	-3.419420090286125E+00
(d)	445	1574	2.79E-04	1.17E-05	-3.586671224186048E+00
Adaptive subdivision with tolerance 10^{-5}					
(a)	559	1960	9.44E-05	3.59E-07	-1.234462106679414E+00
(b)	589	2072	7.73E-05	9.14E-07	-2.087561495861009E+00
(c)	727	2574	9.79E-05	7.81E-07	-3.419560736761150E+00
(d)	923	3222	3.02E-05	6.09E-07	-3.585779065300728E+00

Another integration domain Ω is shown in Fig. 4.1 with six initial quadrilateral elements. The coordinates of the ten vertices are $(0,0.5)$, $(0.1,0)$, $(0.8,0.2)$, $(1,0.85)$, $(0.6,0.8)$, $(0.4,1)$, $(0.3,0.3)$, $(0.7,0.3)$, $(0.7,0.6)$, $(0.3,0.6)$. The singular point is $P_0 = (0.5,0.45)$ and the test functions $f_i, i = 1,\ldots,4$ are given in Table 4.1.

The Table 4.4 shows the results when the adaptive algorithm stops with tolerance 10^{-4}, where 'Step-Err' and 'Approximate Value' are defined as in Table 4.3. The Fig. 4.2 presents meshes and nodes when the adaptive procedure stops for the considered test functions.

All computations were carried out by Matlab ([13]).

In conclusion, we can remark the following further advantage of the proposed approach. By (3.9), the finite part integral I is approximated by the sum of four regular integrals $\tilde{I}_{1,1}^{(k)}$, $\tilde{I}_{1,2}^{(k,\delta)}$, $\tilde{I}_2^{(\delta)}$, $I_{1,3}$, where the first three are $2D$ integrals. By Eqs. (3.4), (3.7) and (3.8), $\tilde{I}_{1,1}^{(k)}$, $\tilde{I}_{1,2}^{(k,\delta)}$, $\tilde{I}_2^{(\delta)}$ are the same kind of cubature on quadrangle with the same kind of nodes, i.e., the eight boundary nodes on the quadrangle, as shown in Fig. 2.1(a). It means that we can use only one procedure to evaluate the three integrals

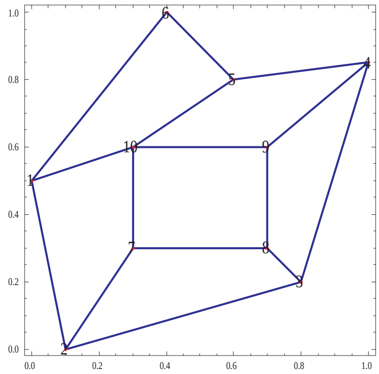

Fig. 4.1 A non-convex domain Ω with initial quadrilateral elements.

Table 4.4 Ω is the polygon given in Fig. 4.1, $P_0 = (0.5, 0.45)$.

Adaptive subdivision with tolerance 10^{-4}				
f	EleN	NodN	Step-Err	Approximate Value
f_1	563	1988	2.09E-05	-3.015424731852383E-01
f_2	601	2054	1.03E-05	1.804458159572488E+00
f_3	661	2172	6.90E-05	5.786696849043063E+00
f_4	967	3474	3.03E-05	5.666572548642983E-01

just with different cubature weights (3.6) and (2.4) according to the integrands in (3.4), (3.7) and (3.8). Besides, the computational cost, equivalent to the number of nodes, can be easily obtained as that one of regular integration. In fact, the proposed algorithm for finite part integrals is compatible and consistent with the algorithms for regular cases presented in [4, 5]. Therefore, it is easy to extend the approach to other cases of singular integrals and by cubatures of high accuracy defined on various kinds of elements. This topic will be discussed in our future work.

Acknowledgements

The authors thank the University of Torino for its support to WWS - World Wide Style Project. The first author also thanks the National Natural Science Foundation of China (Nos. 60533060, 10726067) for their support to his research.

The authors are grateful to the reviewers for their constructive suggestions and comments.

References

1. Dagnino, C., Lamberti, P.: Finite part integrals of local bivariate C^1 quasi-interpolating splines. Approx. Theory & Appl. **16** 68-79 (2000)
2. Farin, G.: Triangular Bernstein-Bézier patches. Computer Aided Geometric Design **3** 83-127 (1986)
3. Li, C.J., Wang, R.H.: A new 8-node quadrilateral spline finite element. J. Comp. Appl. Math. **195** 54-65 (2006)

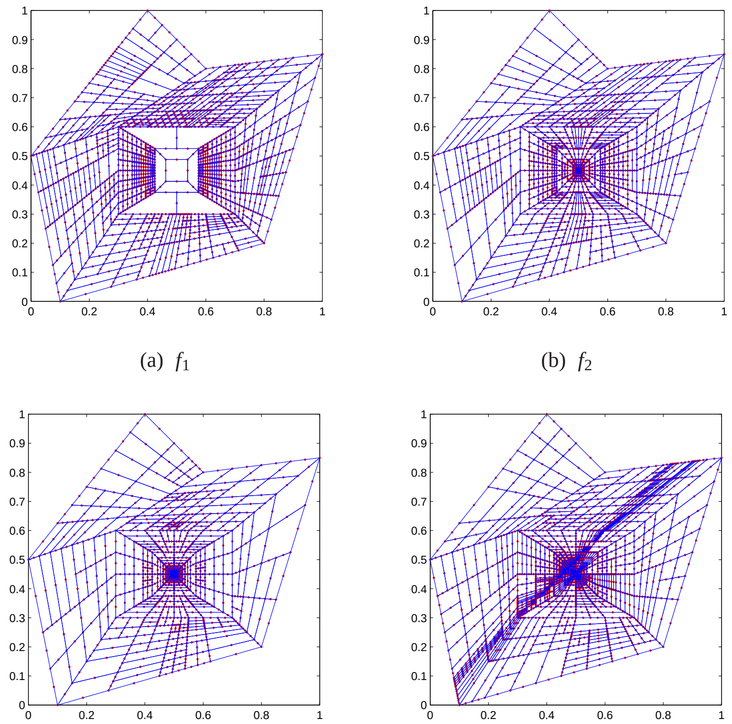

(a) f_1 (b) f_2

(c) f_3 (d) f_4

Fig. 4.2 Meshes and nodes when the adaptive procedure stops.

4. Li, C.J., Dagnino, C.: An adaptive numerical integration algorithm for polygons. Appl. Num. Math. (2009, accepted, doi:10.1016/j.apnum.2009.11.001)
5. Li, C.J., Lamberti, P., Dagnino, C.: Numerical integration over polygons by an 8-node quadrilateral spline finite element. J. Comp. Appl. Math. **233** 279-292 (2009)
6. Monegato, G.: The numerical evaluation of a 2-D Cauchy principal value integral arising in boundary integral equation methods. Math. Comp. **62** 765-777 (1994)
7. Monegato, G.: Numerical evaluation of hypersingular integrals. J. Comp. Appl. Math. **50** 9-31 (1994)
8. Monegato, G.: Definitions, properties and aplications of finite-part integrals. J. Comp. Appl. Math. **229** 425-439 (2009)
9. Theocaris, P.S., Ioakimidis, N.I., Kazantzakis, J.G.: On the numerical evaluation of two-dimensional principal value integrals. Intern. J. Numer. Methods Engrg. **14** 629-634 (1980)
10. Tricomi, F.: Equazioni integrali contenenti il valor principale di un integrale doppio. Math. Zeit. **27** 87-133 (1928)
11. Wang, R.H., Lu, Y.: Quasi-interpolating operators and their applications in hypersingular integrals. J. Comp. Math., **16** 337-344 (1998)
12. Zienkiewicz, O.C., Taylor, R.L.: The finite element method, fifth ed. Elsevier (Singapore) Pte ltd. (2005)
13. The MathWorks, Matlab, The Language of Technical Computing, Version 7.5, 2007, www.mathworks.com/
14. Wolfram Research, Mathematica, Version 5.1, 2004, www.wolfram.com/